Journal of Electroanalytical Chemistry 662 (2011) 143–149

Contents lists available at ScienceDirect

Journal of Electroanalytical Chemistry

journal homepage: www.elsevier.com/locate/jelechem

# Electrochemical Impedance Spectroscopy (EIS) of ion sensors Direct modeling and inverse problem solving using the Nernst–Planck–Poisson (NPP) model and the HGS(FP) optimization strategy

B. Grysakowski [a], J.J. Jasielec [b], B. Wierzba [a], T. Sokalski [b,*], A. Lewenstam [a,b], M. Danielewski [a]

[a] AGH – University of Science and Technology, Faculty of Material Science and Ceramics, Al. Mickiewicza 30, 30059 Cracow, Poland
[b] Process Chemistry Centre, c/o Centre for Process Analytical Chemistry and Sensor Technology (ProSens), Åbo Akademi University, Biskopsgatan 8, 20500 Åbo-Turku, Finland

ARTICLE INFO

*Article history:*
Available online 23 May 2011

*Keywords:*
Inverse method
Genetic algorithm
Nernst–Planck–Poisson model
EIS
ISE
Simulation

ABSTRACT

The Nernst–Planck–Poisson (NPP) model is used to numerically simulate electrochemical impedance spectra (EIS) of ion-selective electrodes (ISEs). By using the Hierarchical Genetic Strategy with real number encoding (HGS(FP)) the reverse problem is solved. The NPP–HGS(FP) method allows estimation of physicochemical parameters of ISEs with plastic membranes, which is illustrated here by using NPP–HGS(FP) for obtaining the values of the diffusion coefficients of ions in the ISE membrane phase.

The NPP–HGS(FP) method allows calculation of the most accurate solution of the inverse problem and can be effectively used to facilitate the process of finding the parameters for optimal ISE performance.

The method presented here not only allows for interpretation of the EIS spectra but also for accounting for the mechanism of the processes occurring at the interface in terms of physicoelectrochemically valid concepts.



## 1. Introduction

Electrochemical Impedance Spectroscopy (EIS) is of great importance in the analysis of electrochemical systems, e.g. electrode kinetics, double-layer studies, batteries, corrosion, and membranes in analytical chemistry [1,2]. This technique is based on the disturbance of the electrochemical reaction from its steady state by applying a small perturbation to the system (e.g. sinusoidal, step-function excitation signal) and allows the identification of electrochemical processes occurring in the analyzed system. Quantitative analysis of impedance spectra is predominantly based on the equivalent circuits technique or its modification, the electrical networks method used for instance in the SPICE software [3].

In the equivalent circuits technique a circuit is constructed from simple passive electrical elements (i.e. capacitors, resistors, constant-phase elements, etc.). The main disadvantage of this method is the lack of uniqueness of the equivalent circuit. This clearly stated by IUPAC: "It is definitely wrong to analyze experimental impedance data by just fitting it to an equivalent circuit corresponding to a trial and error. The reason for this is that the impedance response of several equivalent circuits can follow exactly the same function of frequency, only with different meanings of the corresponding elements. In addition, a fit will always be successful if an unlimited number of parameters is admitted. Without having an a priori model, the meaning of these parameters is undefined." [4]. The selected circuit represents an analogy to the system in question and does not strictly derive from its physicochemical properties as is the case for the non-equivalent circuit methods, as was accurately emphasized by Macdonald [5].

A much less frequent and more complex approach is the use of physically relevant models. Examples of such approaches were presented for metal/solution electrochemistry using RTD and/or LSV [6,7]. Using the electro-neutrality assumption, these authors developed solutions of diffusion–migration equations coupled with a description of electrochemical reactions occurring at the surface of the metal electrode. Both models make it possible to calculate the complex impedance of the solution/metal system. Tribollet and Newman [6] compared their analytically derived solution with experimental results. On the other hand, Dan et al. [7] compared his analytically derived solutions with his own simulation results.

The aim of this work is to implement a modern inverse method by combining the Nernst–Planck–Poisson (NPP) initial boundary-value problem with the Hierarchical Genetic Strategy with real number encoding (HGS(FP)) in order to obtain optimal parameters (exemplified here by diffusion coefficients) for ion-selective electrodes (ISEs).

This method (NPP–HGS(FP)) allows us to calculate the full time response and impedance spectra of ISEs without approximate assumptions, e.g. the linear dependence of the potential. The

* Corresponding author. Tel.: +358 2 215 4418.
*E-mail address:* tomasz.sokalski@abo.fi (T. Sokalski).

1572-6657/$ - see front matter © 2011 Elsevier B.V. All rights reserved.
doi:10.1016/j.jelechem.2011.04.026

application of the NPP model directly relates the simulated impedance spectra to the physicochemical parameters of the system.

The NPP model coupled with the HGS(FP) algorithm was successfully used [8] for optimization of ISE parameters, e.g. diffusion coefficients, concentrations of ions in the internal solution, and measuring time in order to improve the detection limit of ion-selective electrodes.

## 2. NPP model

There is a great number of papers devoted to the application of the NPP system of equations in membrane electrochemistry. Most of them present steady-state analytical solutions restricted to only one type of system and/or fixed number of species, e.g. derived for liquid ionic exchanger [9–13], or neutral carrier membranes [14,15] where authors developed inter alia the analytical solution for complex impedance of such membrane.

The application of the time dependent NPP model to membrane electrochemistry has been presented in a seminal paper [16]. The authors developed an efficient finite difference scheme, totally implicit in time. The resulting set of non-linear algebraic equations was solved using the Newton–Raphson method.

An approach, based upon this idea and dedicated to the general description of ISE behavior, was later developed [17–20].

The first extension of the NPP model for a two layer system was presented in [21]. The first NPP model implementation where the method of lines (MOL) [22] was used was presented in [23,24]. Later on, MOL extensions of the NPP model for an arbitrary number of layers were developed and implemented in C++ [25] in MathCad [20] and in Matlab [26].

The method introduced in [16] and presented in this paper, gives the opportunity to follow the changes of concentrations of species and membrane potential in time and space for an unlimited number of ionic and neutral species and for multilayer systems [27] and to calculate the complex impedance of such systems [24,26]. Two last papers present the brief discussion of the behavior of the NPP model, mainly the influence of the parameters of the systems on the shape of simulated impedance spectra.

The Nernst–Planck–Poisson model is an initial-boundary value problem that for one dimension is given by the set of equations briefly described below. Let us consider a flat, isotropic membrane with a constant thickness $d$, bathed by two solutions, Fig. 1 [17,18].

The ionic fluxes are expressed by Nernst–Planck equation [28–31]:

$$J_i(t,x) = -D_i\left[\frac{\partial c_i(t,x)}{\partial x} - z_i c_i(t,x)\frac{F}{R\cdot T}E(t,x)\right] \tag{1}$$

where $J_i(t,x)$ is the flux of the $i$th ion, $D_i$ is constant self diffusion coefficient of the $i$th ion, $c_i(t,x)$ is concentration of the $i$th ion, $z_i$ is valence of the $i$th ion, and $E(t,x)$ is electric field strength. $F$ is Faraday constant, $R$ and $T$ denote gas constant and absolute temperature.

The evolution of the electric field is represented by the Poisson equation, which combines the concentration of ions with the resulting electric field strength. Assuming that $\varepsilon$ = const:

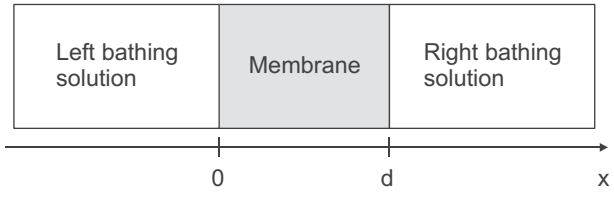


**Fig. 1.** Schematic representation of the considered system.

$$\frac{\partial E(t,x)}{\partial x} = \frac{\rho(t,x)}{\varepsilon} \tag{2}$$

where $\rho(t,x) = F\cdot\sum_i z_i c_i(t,x)$ is the charge density and $\varepsilon$ is dielectric permittivity.

The mass conservation law describes the concentration changes in space and time:

$$\frac{\partial c_i(t,x)}{\partial t} = -\frac{\partial J_i(t,x)}{\partial x} \tag{3}$$

Following [32], the Poisson equation is replaced by its equivalent form, the total current equation

$$I(t) = F\cdot\sum_{i=1}^{r} z_i J_i(t,x) + \varepsilon\frac{\partial E(t,x)}{\partial t} \tag{4}$$

The presence of the displacement current $(\partial E(t,x)/\partial t)$ term allows us to employ the method of lines and to obtain a standard ODEs system, as well as to use the Rosenbrock or Radau integration scheme. The use of the Poisson equation leads to the system of differential–algebraic equations and will force the employment of much more sophisticated and complex numerical methods in order to solve this problem. It is easier to implement the function that describes the perturbation current signal as well (Eqs. (7) and (12) in the following section of this paper).

Fluxes of ions at membrane interfaces are given by Chang–Jaffe boundary conditions [33]:

$$\begin{aligned} J_i(t,0) &= \overrightarrow{k_i^L}c_{i,L} - \overleftarrow{k_i^L}c_i(t,0) \\ J_i(t,d) &= \overrightarrow{k_i^R}c_i(t,d) - \overleftarrow{k_i^R}c_{i,R} \end{aligned} \tag{5}$$

where $\overrightarrow{k_i^L}, \overrightarrow{k_i^R}, \overleftarrow{k_i^L}, \overleftarrow{k_i^R}$ are heterogeneous rate constants at interfaces, where subscript $i$ denotes the component; arrows – direction of ion permeation; $L$ and $R$ are the left and right boundary of the membrane, respectively. $c_{i,L}$, $c_{i,R}$ denotes concentrations of the $i$th ion in the left and right bathing solutions. The concentrations of ions and the electric field strength values at the boundaries of the membrane change with time, but the ionic concentration values in both left and right solutions remain constant. Initial concentrations obey the electro-neutrality condition and, consequently, there is initially no space charge in the membrane: $c_i(0,x) = c_i^0(x)$, $E(0,x) = 0$ for $x \in [0, d]$.The membrane potential, $V$, is given by:

$$V(t) = -\int_0^d E(t,x)dx \tag{6}$$

In the NPP model the potential is calculated across the entire system and not divided arbitrarily into the boundary and diffusion parts.

Eqs. (1)–(5) were converted into a finite difference scheme with the space grid containing closely spaced points near the interfaces and a distinctively wider spacing inside the membrane. The problem is further simplified by assuming constant diffusion coefficients and dielectric permittivity. The system of equations presented above was converted into the system of ordinary differential equations by using the method of lines. This operation allowed us to use an integration scheme in order to solve numerically the NPP problem. Owing to the stiffness of the obtained system of ODE, numerical integrators such as Rosenbrock or Radau were used. The MOL numerical technique we used to solve the NPP problem differs from the one used in the seminal paper by Brumleve and Buck [16] in that it is faster and more efficient. This difference is, however, of minor importance. The novel approach is the combination of a relevant physicochemical model (NPP) and a sophisticated search strategy (HGS-FPP) to solve the inverse problem.

## 3. Electrochemical Impedance Spectroscopy

The impedance of a system can be determined from the linear response of the system to a small-current perturbation. In this paper, two methods of calculation are used to obtain the real and imaginary part of the complex impedance. In the first method, based on the approach described in [16], a system which has reached steady-state is disturbed by a current with a current density described by Heavyside's function:

$$I(t) = \begin{cases} 0 & t < 0 \\ \Delta I & t \geqslant 0 \end{cases} \tag{7}$$

In the next step, the potential-time response of the system is transformed into a frequency domain with the use of the Fourier transform and approximation of the integrals by the trapezoid rule:

$$\begin{aligned} V'(\omega) &= \sum_k \Delta V'_k \\ V''(\omega) &= \sum_k \Delta V''_k + V_\infty/\omega \end{aligned} \tag{8}$$

$$\begin{aligned} \Delta V'_k = {} & (V(t_{k+1}) - V(t_k))(\cos\omega t_{k+1} - \cos\omega t_k)/\omega^2(t_{k+1} - t_k) \\ & + (V(t_{k+1}) - V_\infty)\sin\omega t_{k+1} - (V(t_k) - V_\infty)\sin\omega t_k)/\omega \end{aligned} \tag{9}$$

$$\begin{aligned} \Delta V''_k = {} & (V(t_{k+1}) - V(t_k))(\sin\omega t_{k+1} - \sin\omega t_k)/\omega^2(t_{k+1} - t_k) \\ & + (V(t_{k+1}) - V_\infty)\cos\omega t_{k+1} - (V(t_k) - V_\infty)\cos\omega t_k)/\omega \end{aligned} \tag{10}$$

In this method, only one simulation is needed to calculate the imaginary and real parts of the complex impedance for a broad frequency range.

$$\begin{aligned} Z'(\omega) &= -V''(\omega)\cdot\omega/\Delta I \\ Z''(\omega) &= V'(\omega)\cdot\omega/\Delta I \end{aligned} \tag{11}$$

Similar results can be obtained using the second method where the system is perturbed by a sinusoidal excitation signal.

$$I(t) = \begin{cases} 0 & t < 0 \\ \Delta I + I_0\sin(\omega t) & t \geqslant 0 \end{cases} \tag{12}$$

The potential-time response of the system is the sinus function given by the following equation:

$$V(t) = \Delta V + V_0\sin(\omega t + \phi) \tag{13}$$

In order to obtain the complex impedance of the system for a given frequency (Eq. (14)), the amplitude of the potential response $V_0$ and the phase angle $\varphi$ must be calculated.

$$\begin{aligned} Z^*(\omega) &= Z'(\omega) + jZ''(\omega) \\ Z'(\omega) &= -\frac{V_0}{I_0}\cos(\phi) \\ Z''(\omega) &= \frac{V_0}{I_0}\sin(\phi) \end{aligned} \tag{14}$$

## 4. HGS(FP)

The HGS(FP) is a genetic optimization technique. Optimization methods are based on searching the best fit ("the most useful" from the error function point of view) individuals from a given population. In contrast, in fitting methods only one set of initial parameters exists. In other words, optimization is a process of testing the population (group) of individuals, which has been created at the beginning of the algorithm (e.g. by the roulette wheel selection method) and what is very important are randomly distributed in the solution's space. This advantage, in contrast to fitting methods, allows all (global as well as local) minima (or maxima) of given error function to be found. Of course, it is possible to control the population and this can be realized with the use of genetic algorithms. It is worth emphasizing that fitting methods are unable to find all extrema of the error function and it happens very often that the fitting algorithm is terminated in one of the local minimum/maximum of the error function.

The main advantages of genetic algorithms are: (1) The ability to search for the most optimal solutions of error functions with multiple extrema. Non-stochastic (deterministic) methods usually fail to find global minimum/maximum of such an error function. (2) Due to the random distribution of individuals in the solution's space it is possible to scan a vast interval of values of optimized parameters. (3) Genetics operations allow new individuals (crossover) to be created, as well as moving them (mutation) into new points of the solution's space and scanning new areas. (4) The method allows all minima/maxima of a given error function– global and local optima of this function to be found. (5) They are independent of the shape of the error plane. For example the Simplex method is most efficient when the shape of error function mimics a "well". (6) In contrast to gradient methods, there is no need to use derivatives of the goal/error function. This advantage allows searching extrema of the discontinuous functions.

Such algorithms are of interest in many areas. Genetic algorithms are highly efficient when solving problems with many optima [34,35]. The Hierarchical Genetic Strategy introduced in 2000 [36], and further generalized [37] by the introduction of the floating point encoding, is one such efficient algorithm. The introduction of the genetic operators, mutation and crossover, in floating point representation improves the efficiency of the optimization strategy. The HGS accuracy and low computational cost for multimodal benchmarks was shown in [37].

The efficiency, i.e. the low computational cost and effectiveness of HGS(FP) in finding global optima (maxima or minima), results from the concurrent search in the optimization space by many small populations of individuals (solutions) [35,38]. The creation of these populations is governed by genetic processes with low complexity [37]. Unlike the majority of genetic algorithms, the main engine of the HGS(FP) is based on real-number encoding. The genetic operators are: (1) mutation (i.e. the genotype perturbation of the "parent" individual) which allows random relocation of the individuals in the environment (optimization space), and (2) the arithmetic crossover, which is quasi-deterministic. The resulting genotype is a combination of the "parent" genotypes. The real number encoding used in HGS(FP) is much more efficient than the binary encodings (0, 1 codes) which are usually used. Its efficiency is due to the conservation of the natural (topological) space where all variables are real numbers.

The main engine of the Hierarchical Genetic Strategy with real number encoding runs a set of evolutionary processes [39,40]. In each evolving step, the algorithm creates a new population which is searched for optima with higher precision. The two genetic operators for floating point representation are given by:

(1) crossover (generation of a new individual between two already existing ones):

$$Y_i = X_i^1 + \mathcal{N}(mean, \sigma)(X_i^2 - X_i^1), \quad i = 1, \ldots, N \tag{15}$$

(2) mutation (generation of a new individual based on already existing ones):

$$Y_i = X_i^1 + (\mathcal{N}(0, \sigma))_i, \quad i = 1, \ldots, N \tag{16}$$

where $Y_i$ denotes a new individual generated by a crossover or mutation operation, $X_i^1$ and $X_i^2$ are parent individuals, $\mathcal{N}(mean, \sigma)$

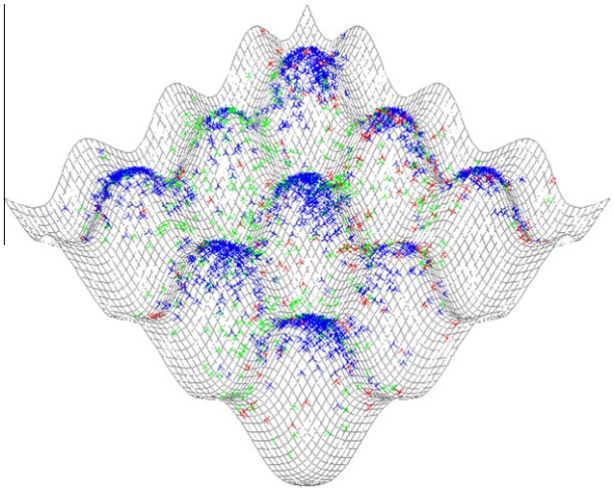

**Fig. 2.** The example results obtained with the HGS(FP) strategy for the 2-dimensional test function $f(x,y) = \cos(5\pi x) + \cos(5\pi y) + x^2 + y^2, \quad x,y \in [-0,7;0,7]$. Points denote the phenotypes of the population.

denotes the normally distributed random variable, where *mean* is a random number and $\sigma$ its variation, respectively.

In order to generate a new population, the classical roulette selection is used. The probability, Pr $(X)$, of obtaining an individual $X$ from the population $P$, $(X \in P)$ is:

$$\Pr(X) = \frac{fitness(X)}{\sum_{Y \in P} fitness(Y)}, \quad \forall\, X \in P \tag{17}$$

where *fitness*$(X)$ is an estimation of the adaptation of the $X$th individual (the value of the goal function).

As an example, the results obtained with the HGS(FP) method for a 2-dimensional test function $(f(x,y) = \cos(5\ \pi\ x) + \cos(5\ \pi\ y) + x^2 + y^2, \quad x,y \in [-0,7;0,7])$ are shown in Fig. 2. This function is a generally accepted test function used to compare and evaluate different algorithms. The objective was to find all of the function maxima.

The points on the mesh show the phenotypes of the populations. As can be seen, all of the maxima (local and global) are found.

Incidentally, the parallel version of HGS provides for a decrease in the computation time [39].

## 5. NPP–HGS(FP) method

The presented work is not the first one devoted to applications of genetic algorithms in electrochemistry. In contrast to other papers [41–44], we use basic physical laws and well known electrochemical expressions, and solve them numerically in the time and space domain. In [42] the authors use the simplest form of genetic algorithm (SGA) in order to create a population of initial parameters of elements of equivalent circuits for further calculations with the use of the non-linear regression procedure. The method we use allows us to omit the necessity of deriving an analytical function that describes the complex impedance of the system under consideration, as well as the analysis of equivalent circuits and the use of a parameter related to equivalent circuits (e.g. charge transfer resistance, double layer capacitance, etc.). Instead, the NPP–HGS(FP) method shows the direct relation between the physicochemical parameters (e.g. diffusion coefficients, concentrations of species, membrane thickness) of the system with the ISE and the responses of this kind of electrode (e.g. calibration curve [8], potential-time response), as well as the influence of these quantities on the shape of the impedance spectrum and on the impedance values.

Using the HGS(FP) strategy to find the optimal parameters, we reformulate the NPP problem into the optimization one (finding extremes). The problem is now to find the NPP parameters which minimize the difference between the reference (experimental) and calculated (NPP) impedance spectra i.e. to minimize the metric sum, Eq. (18).

$$Erf = \sum_j g^j \left| \mathrm{Re}\left(Z^j_{calc}\right) - \mathrm{Re}\left(Z^j_{\exp}\right) \right| + \sum_j h^j \left| \mathrm{Im}\left(Z^j_{calc}\right) - \mathrm{Im}\left(Z^j_{\exp}\right) \right| \tag{18}$$

where $g^j$, $h^j$ are weight functions, $Z^j_{calc}$, $Z^j_{\exp}$ are calculated and experimental complex impedance values at the $j$th frequency.

The presented method allows us to find parameters such as membrane thickness, dielectric permittivity, diffusion coefficients and concentrations (in the internal reference solution and in the sample) of all components, as well as the heterogeneous rate constants.

All the results presented here were obtained with the use of the NPP model implemented in Matlab coupled with the HGS(FP) method implemented in C++.

## 6. Numerical experiments and results

In order to investigate the behavior of the employed algorithm (NPP–HGS(FP)) we used a well defined system described by the physicochemical parameters given in Tables 1 and 3. The EIS spectra for this system were calculated using the NPP model and the excitation signals given by Eqs. (7) and (12). To these spectra, different levels of noise (0%, 7%, 15%, 30%) were added according to the following equations:

**Table 2**
The reference and approximated diffusion coefficients by the NPP–HGS(FP) method.

| | Diffusion coefficients $D_i$ (m$^2$ s$^{-1}$) | | |
|---|---|---|---|
| | Reference value | NPP–HGS(FP) approximation | |
| | | First run | Second run |
| $A^{2+}$ | $10^{-11}$ | $1.006 \times 10^{-11}$ | $0.954 \times 10^{-11}$ |
| $B^+$ | $0.7 \times 10^{-11}$ | $0.75 \times 10^{-11}$ | $0.715 \times 10^{-11}$ |
| $X^-$ | $0.5 \times 10^{-11}$ | $0.499 \times 10^{-11}$ | $0.595 \times 10^{-11}$ |

**Table 1**
Initial concentrations, diffusion coefficients and heterogeneous rate constants used in the first numerical experiment. $\varepsilon_r = 4$, $d = 2 \times 10^{-4}$ m. $c_{iM}$ denotes the initial uniform concentration of the $i$th ion in the membrane phase.

| | $c_{iL}$ $(M)$ | $c_{iM}$ $(M)$ | $c_{iR}$ $(M)$ | $D_i$ (m$^2$ s$^{-1}$) | $\overrightarrow{k_i^I}$ (m s$^{-1}$) | $\overleftarrow{k_i^I}$ (m s$^{-1}$) | $\overrightarrow{k_i^R}$ (m s$^{-1}$) | $\overleftarrow{k_i^R}$ (m s$^{-1}$) |
|---|---|---|---|---|---|---|---|---|
| $A^{2+}$ | $10^{-2}$ | $5 \times 10^{-4}$ | 1 | $10^{-11}$ | $10^{-3}$ | $10^{-3}$ | $10^{-3}$ | $10^{-3}$ |
| $B^+$ | 0.15 | 0 | 0 | $0.7 \times 10^{-11}$ | $4.472 \times 10^{-7}$ | $10^{-3}$ | $10^{-3}$ | $4.472 \times 10^{-7}$ |
| $X^-$ | 0 | $10^{-3}$ | 0 | $0.5 \times 10^{-11}$ | 0 | 0 | 0 | 0 |

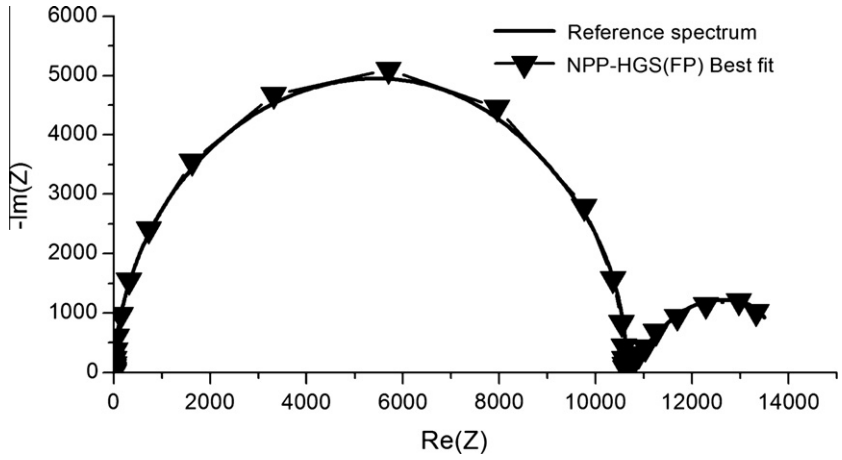


**Fig. 3.** The results of NPP–HGS(FP) compared with the reference spectrum calculated for different values of diffusion coefficients for each ion.

**Table 3**
Initial concentrations, diffusion coefficients and heterogeneous rate constants used in the second numerical experiment. $\varepsilon_r = 4$, $d = 2 \times 10^{-4}$ m. $c_{iM}$ denotes the initial concentration of the $i$th ion in the membrane phase. $c_{iM}$ denotes the initial uniform concentration of the $i$th ion in the membrane phase.

| | $c_{iL}$ $(M)$ | $c_{iM}$ $(M)$ | $c_{iR}$ $(M)$ | $D_i$ $(m^2\ s^{-1})$ | $\overrightarrow{k_i^L}$ $(m\ s^{-1})$ | $\overleftarrow{k_i^L}$ $(m\ s^{-1})$ | $\overrightarrow{k_i^R}$ $(m\ s^{-1})$ | $\overleftarrow{k_i^R}$ $(m\ s^{-1})$ |
|---|---|---|---|---|---|---|---|---|
| $A^{2+}$ | $10^{-2}$ | $5 \times 10^{-4}$ | 1 | $10^{-11}$ | $10^{-3}$ | $10^{-3}$ | $10^{-3}$ | $10^{-3}$ |
| $B^+$ | 0.15 | 0 | 0 | $10^{-11}$ | $4.472 \times 10^{-7}$ | $10^{-3}$ | $10^{-3}$ | $4.472 \times 10^{-7}$ |
| $X^-$ | 0 | $10^{-3}$ | 0 | $10^{-11}$ | 0 | 0 | 0 | 0 |

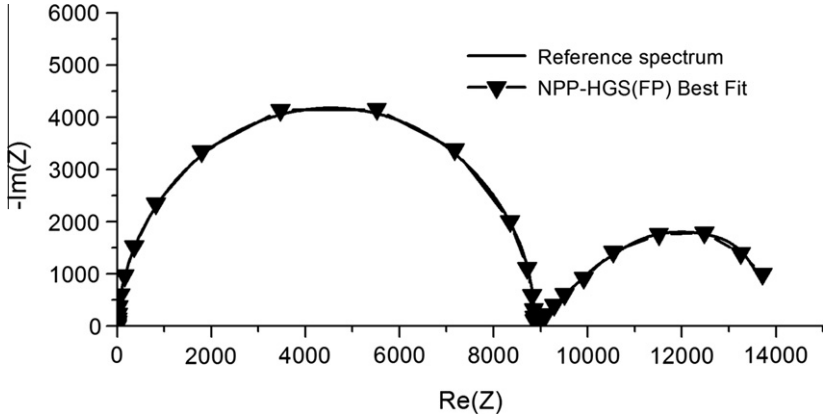


**Fig. 4.** The results of NPP–HGS(FP) compared with the reference spectrum calculated for equal values of diffusion coefficients for each ion. Reference spectrum with no added noise.

$$\begin{aligned} &\mathrm{Re}(Z)^* = \mathrm{Re}(Z) + a \cdot N \cdot \mathrm{Re}(Z) \\ &\mathrm{Im}(Z)^* = \mathrm{Im}(Z) + b \cdot N \cdot \mathrm{Im}(Z) \\ &a \in [0,1] \\ &b \in [0,1] \\ &N \in \{0, 0.07, 0.15, 0.30\} \end{aligned} \tag{19}$$

where $a$ and $b$ are random numbers from [0, 1] interval. $N$ denotes the level of added noise.The resulting impedance spectra, with the added noise, were used as virtual experiment data (reference spectra) to test the NPP–HGS(FP) algorithm. The aim was to obtain the original physicochemical parameters used to generate the spectra.

In the first virtual experiment, based on the reference spectrum obtained with the data presented in Table 1, we tried to reproduce diffusion coefficient values. In this system, every ion has a different diffusion coefficient. For all diffusion coefficients, a search range between $10^{-13}$ and $10^{-9}$ $m^2\ s^{-1}$ was used.

The simulations show that the diffusion coefficient of $B^+$ has little effect on the shape of the impedance spectrum. The results of the NPP–HGS(FP) simulations are presented in Table 2 and Fig. 3. They demonstrate clearly, that HGS(FP) method is the stochastic one. Diffusion coefficients calculated during two successive runs have different values, but still remain close to the reference values.

The aim of the second numerical experiment was to mimic the real experimental conditions, i.e. different levels of noise (0%, 7%, 15% and 30%) were artificially added to the reference spectrum (Eq. (19)). In this system, the diffusion coefficients of all the ions are equal (Table 3).

The basic reference spectrum, the spectra with the added noise and the best fits obtained using the NPP–HGS(FP) method are shown in Figs 4–7. The values of the approximated diffusion coefficients are shown in Table 4.

The obtained results show good agreement between the reference values (obtained with the use of virtual experiment)

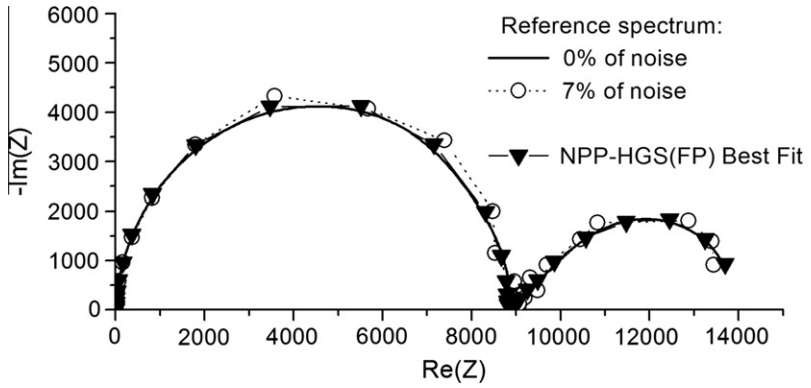


**Fig. 5.** The results of NPP–HGS(FP) compared with the reference spectrum with 7% of noise.

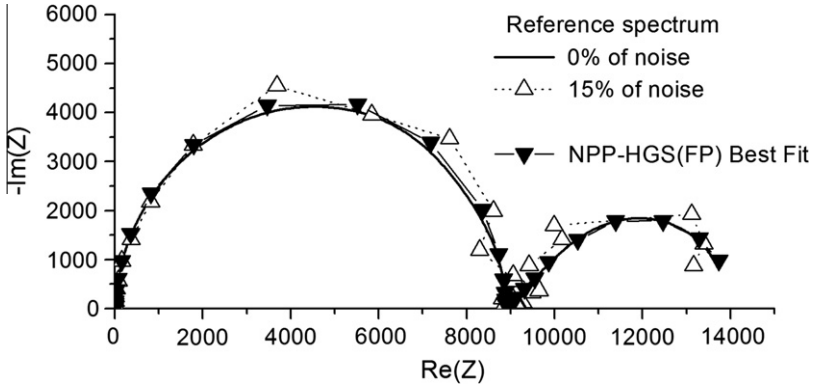


**Fig. 6.** The results of NPP–HGS(FP) compared with the reference spectrum with 15% of noise.

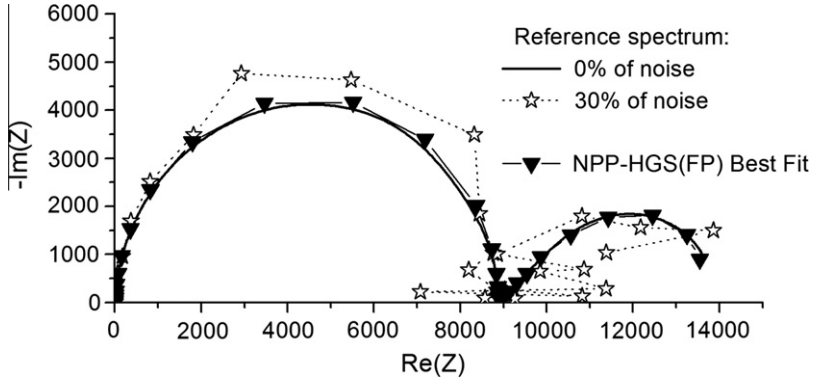


**Fig. 7.** The results of NPP–HGS(FP) compared with the reference spectrum with 30% of noise.

**Table 4**
The reference and approximated diffusion coefficients by the NPP–HGS(FP) method.

| | Diffusion coefficients $D_i$ ($m^2\ s^{-1}$) | | | | |
|---|---|---|---|---|---|
| | Reference value | 0% of noise | 7% of noise | 15% of noise | 30% of noise |
| $A^{2+}$ | $10^{-11}$ | $0.9\ (99) \times 10^{-11}$ | $0.989 \times 10^{-11}$ | $0.9\ (99) \times 10^{-11}$ | $0.9\ (99) \times 10^{-11}$ |
| $B^{+}$ | $10^{-11}$ | $1.0096 \times 10^{-11}$ | $0.9\ (99) \times 10^{-11}$ | $0.99998 \times 10^{-11}$ | $0.9804 \times 10^{-11}$ |
| $X^{-}$ | $10^{-11}$ | $1.0059 \times 10^{-11}$ | $0.9\ (99) \times 10^{-11}$ | $0.9\ (99) \times 10^{-11}$ | $0.9\ (99) \times 10^{-11}$ |

and the calculated values (NPP–HGS(FP) method) of the diffusion coefficients. Even for the reference spectra calculated for a system with different diffusion coefficients for each ion, as well as with a high level of noise, the NPP–HGS(FP) method found the expected solution. In all cases, the deviation from the expected result was less than 1%.

The ultimate challenge for the NPP–HGS(FP) method will be to find the correct values in the case where all ions have different diffusion coefficients and the spectrum contains a high level of noise.

## 7. Conclusions

It is shown that by applying the NPP and HGS the EIS spectra could be a source for physicochemical characteristic of ISEs. This gives a new possibility to assess the physicochemical properties of the ISEs used and to access their response mechanism.

Two methods for generating impedance spectra using the NPP–HGS(FP) method were presented. The results obtained by these methods are in the good agreement.

Calculating the ISE parameters from the EIS spectra, both without noise and in the presence of an increasing amount of experimental noise, gave approximately the same results. The NPP–HGS(FP) method can be used to obtain meaningful values of diffusion coefficients in the ISE membrane even in experimental conditions where the noise level is high.

The methods of EIS spectra interpretation based on physical models are superior to the methods based on equivalent circuits in the sense that they not only aim at reproducing the phenomenon of interest but also at accounting for the mechanism of the processes occurring at the interface in terms of physico-electrochemically valid concepts.

## Acknowledgments

Financial support from the Graduate School of Chemical Engineering (Finland) and the Finnish Funding Agency for Technology and Innovation (TEKES), the IMO Intelligent Monitoring for Health and Well-being (IMO) SHOK program are gratefully acknowledged.

## References

[1] C. Gabrielli, in: I. Rubinstein (Ed.), Physical Electrochemistry: Principles, Methods and Applications, Marcel Dekker, New York, 1995, pp. 243–292.
[2] C. Gabrielli, M. Keddam, P. Rousseau, V. Vivier, in: COMSOL Multiphysics User's Conference, Paris, 2005.
[3] R. Naumann, D. Walz, S.M. Schiller, W. Knoll, Journal of Electroanalytical Chemistry 550 (2003) 241–252.
[4] M. Sluytersrehbach, Pure and Applied Chemistry 66 (1994) 1831–1891.
[5] D.D. Macdonald, Electrochimica Acta 51 (2006) 1376–1388.
[6] B. Tribollet, J. Newman, Journal of the Electrochemical Society 131 (1984) 2780–2785.
[7] C. Dan, B. Van den Bossche, L. Bortels, G. Nelissen, J. Deconinck, Journal of Electroanalytical Chemistry 505 (2001) 12–23.
[8] J.J. Jasielec, B. Wierzba, B. Grysakowski, T. Sokalski, M. Danielewski, A. Lewenstam, Novel strategy for finding the optimal parameters of ion selective electrodes, ECS Transactions 33 (2011) p.19.
[9] G. Karreman, G. Eisenman, Bulletin of Mathematical Biophysics 24 (1962) 413–427.
[10] F. Conti, G. Eisenman, Biophysical Journal 5 (1965) 511–530.
[11] F. Conti, G. Eisenman, Biophysical Journal 6 (1966) 227–246.
[12] J.L. Walker, G. Eisenman, Biophysical Journal 6 (1966) 513–533.
[13] J.P. Sandblom, G. Eisenman, J.L. Walker Jr., Journal of Physical Chemistry 71 (1967) 3862–3870.
[14] C. Gabrielli, P. Hemery, P. Letellier, M. Masure, H. Perrot, M.I. Rahmi, M. Turmine, Journal of Electroanalytical Chemistry 570 (2004) 275–289.
[15] C. Gabrielli, P. Hemery, P. Letellier, M. Masure, H. Perrot, M.I. Rahmi, M. Turmine, Journal of Electroanalytical Chemistry 570 (2004) 291–304.
[16] T.R. Brumleve, R.P. Buck, Journal of Electroanalytical Chemistry 90 (1978) 1–31.
[17] T. Sokalski, A. Lewenstam, Electrochemistry Communications 3 (2001) 107–112.
[18] T. Sokalski, P. Lingenfelter, A. Lewenstam, Journal of Physical Chemistry B 107 (2003) 2443–2452.
[19] P. Lingenfelter, I. Bedlechowicz-Sliwakowska, T. Sokalski, M. Maj-Zurawska, A. Lewenstam, Analytical Chemistry 78 (2006) 6783–6791.
[20] T. Sokalski, W. Kucza, M. Danielewski, A. Lewenstam, Analytical Chemistry 81 (2009) 5016–5022.
[21] P. Lingenfelter, T. Sokalski, A. Lewenstam, Unbiased Selectivity Coefficients: New Insights From the Nernst–Planck–Poisson Model, Matrafured, Hungary, 2005.
[22] W.E. Schiesser, The Numerical Method of Lines: Integration of Partial Differential Equations, Academic Press, San Diego, 1991.
[23] R. Filipek, Polish Ceramic Bulletin 90 (2005) 103–108.
[24] W. Kucza, M. Danielewski, A. Lewenstam, Electrochemistry Communications 8 (2006) 416–420.
[25] J. Jasielec, Master Thesis, AGH-UST/AAU, 2008.
[26] B. Grysakowski, B. Bozek, M. Danielewski, Diffusion in Solids and Liquids III 273–276 (2008) 113–118.
[27] J.J. Jasielec, T. Sokalski, R. Filipek, A. Lewenstam, Electrochimica Acta 55 (2010) 6836–6848.
[28] W. Nernst, Zeitschrift Fur Physikalische Chemie 2 (1888) 613.
[29] W. Nernst, Zeitschrift Fur Physikalische Chemie 4 (1889) 129.
[30] M. Planck, Annual Review of Physical Chemistry 40 (1890) 561.
[31] M. Planck, Annual Review of Physical Chemistry 39 (1890) 161.
[32] H. Cohen, J.W. Cooley, Biophysical Journal 5 (1965) 145–162.
[33] H.C. Chang, G. Jaffe, Journal of Chemical Physics 20 (1952) 1071–1077.
[34] D. Whitley, S. Rana, R.B. Hackendorn, Island Model Genetic Algorithms and Linearly Separable Problems, AISB 1997 Workshop on Evolutionary Computing, Manchester, 1997.
[35] E. Cantu-Paz, Efficient and Accurate Parallel Genetic Algorithms, Kluwer Academic Publishers., 2000.
[36] J. Kolodziej, R. Gwizdala, J. Wojtusiak, Hierarchical Genetic Strategy as a Method of Improving Search Efficiency, Advances in Multi-agent Systems, Jagiellonian University Press, 2001. pp. 149–161.
[37] A. Semczuk, B. Wierzba, Hierarchical genetic strategy with real number encoding, Krakow, Jagiellonian University, Institute of Computer Science, 2003. (in Polish)
[38] H. Telega, R. Schaefer, E. Cabib, Lecture Notes in Computer Science 1541 (1998) 551–556.
[39] J. Kolodziej, R. Schaefer, A. Paszynska, Journal of Theoretical and Applied Mechanics, Computational Intelligence 42 (2004) 519–539.
[40] R. Schaefer, B. Barabasz, Lecture Notes in Computer Science 5103 (2008) 682–691.
[41] T.J. VanderNoot, I. Abrahams, Journal of Electroanalytical Chemistry 448 (1998) 17–23.
[42] M.L. Yang, X.H. Zhang, X.H. Li, X.Z. Wu, Journal of Electroanalytical Chemistry 519 (2002) 1–8.
[43] M. Maeder, Y.M. Neuhold, G. Puxty, Chemometrics and Intelligent Laboratory Systems 70 (2004) 193–203.
[44] P. Watkins, G. Puxty, Talanta 68 (2006) 1336–1342.